Active noise cancellation by using the linear quadratic Gaussian independent modal space control

Mingsian R. Bai and Chifong Shieh
Department of Mechanical Engineering, National Chiao Tung University, 1001 Ta Hsueh Road, Hsinchu 30050, Taiwan, Republic of China

(Received 1 August 1994; accepted for publication 25 November 1994)

The objective of this study is to develop an active noise controller based on optimal control approaches for enclosed Gaussian noise fields. By independent modal space control, the individual mode in the acoustic field is suppressed by the corresponding modal control exerted by loudspeakers. The formulation of the modal controller is considerably simplified because modal coupling is neglected. For the Gaussian noises considered in this study, the linear quadratic Gaussian algorithm in conjunction with the Kalman–Bucy filter is employed to perform state feedback and estimation. The developed controller is validated by simulations for a duct and a rectangular room. The results indicate that the technique will yield significant noise reduction if one uses the same number of controlled modes, microphones, and loudspeakers. Satisfactory performance is possible if one carefully avoids placing microphones and loudspeakers at the nodal points.

PACS numbers: 43.20.Ks, 43.50.Ki

INTRODUCTION

Noise control for enclosed acoustic fields falls into two categories: the passive approach and the active approach. The former is conventional and is based on some well-developed design methods such as the acoustic filter theory.[1] On the other hand, active noise control (ANC)[2] is based on a principle that one artificially generates an *antifield* to destructively interfere with the undesirable noise field. It provides certain advantages over the passive approach. These attractive features include improved low-frequency performance, reduction of size and weight, zero back pressure, and programmable flexibility of design. Advances are being made toward developing a commercial hybrid active–passive noise controller in which the low-frequency attenuation is provided by an active system, while the high-frequency attenuation is provided by passive hardware. There are many applications of the ANC technique, including silencers for gas pipelines, noise cancelers for air conditioning systems, mufflers for internal combustion engines, noise attenuators for vehicle or airplane cabins, and so forth.[2]

This study focuses primarily on the development of an ANC technique for enclosed Gaussian noise fields, based on the linear quadratic Gaussian (LQG)[3] algorithm in conjunction with independent modal space control (IMSC).[4,5] The analysis is motivated by the formulation of the large space structure (LSS)[6,7] since both systems are of the distributed type and have an infinite number of degrees of freedom. The control actions for LSS may be taken in the actual space as well as in the modal space. The latter approach is adopted in this study due to the simplicity of the controller design. This simplicity stems from uncoupling a continuous system (described by a partial differential equation) into a set of simple oscillators (described by modal ordinary differential equations) via orthogonality of eigenfunctions. In theory, one can control the entire system by controlling the infinite number of modes of the system. In practice, one is only able to control low-frequency modes, e.g., below the Schroeder's cutoff frequency, where modal decomposition is meaningful. The applications of modal control can be found in many areas in structural dynamics, such as beam vibration, flow-induced vibration, airfoil fluttering, and so forth.[6–10]

Among the modal control techniques, the IMSC seeks to control the individual mode of a continuous system by modal controls by neglecting modal coupling. This provides a remarkable reduction of problem size in controller design. However, IMSC requires distributed types of sensors and actuators which are essentially free of spillover effects.[5,11] This poses a problem because the most commonly used transducers in acoustic applications are discrete types, e.g., microphones and loudspeakers. Thus a suitable approximation scheme must be taken to represent the measurement and control actions of the acoustic field by using a finite number of discrete sensors and actuators.

In the design of the modal controller, two techniques are available to accomplish the state feedback. One method is based on pole allocation and the other is based on linear quadratic (LQ) optimal control.[12–14] In this research, the latter is adopted because it not only admits a reasonable balance between the control error and control effort but also yields a stable control system. In addition, if the control system of interest is subjected to stochastic excitations, then the LQG algorithm should be employed. In viewing that the LMS algorithm and its variants are prevailing methods in the ANC community,[2] the LQG-IMSC technique proposed in this paper provides a useful alternative in attenuating noises in enclosures.

A duct and a rectangular room are selected as test cases in a simulation to investigate the effects of various control parameters. The results indicate that the developed technique will yield significant noise reduction if the same number of controlled modes, microphones, and loudspeakers are em-

 0001-4966/95/97(5)/2664/11/$6.00 © 1995 Acoustical Society of America

Redistribution subject to ASA license or copyright; see http://acousticalsociety.org/content/terms. Download to IP: 140.113.38.11 On: Wed, 30 Apr 2014 06:45:39

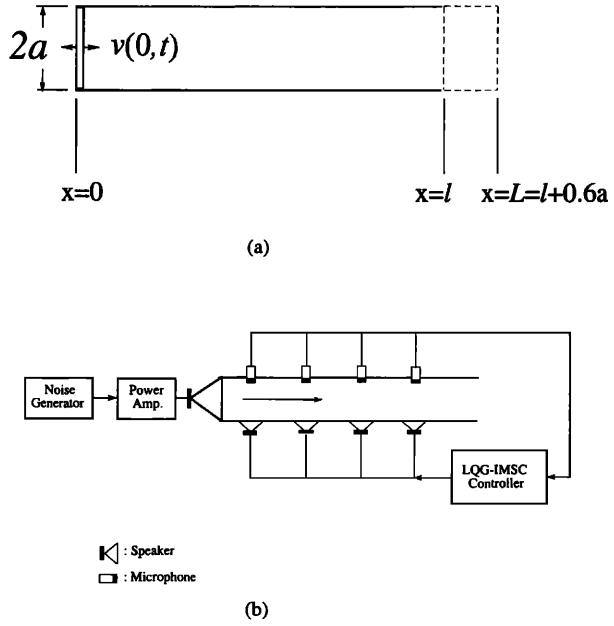

FIG. 1. (a) Schematic diagram of an open-ended duct of length 2 m, driven by a rigid piston; (b) configuration of the LQG-IMSC system for the duct.

ployed. Satisfactory performance is possible if one carefully avoids placing actuators and sensors at the nodal points.

I. THEORY AND METHOD

A. Modal equations of the acoustic fields

In this section, modal equations of a duct and a rectangular room are derived by using the orthogonality of eigenfunctions. For the duct case of Fig. 1, it is assumed that one end of the duct is driven by a rigid piston of surface velocity $v(0,t)$ and the other end is left open with radiation impedance z_n. The surface velocity is assumed to be Gaussian white. Since only the plane waves below the cutoff frequency are of interest, the duct field is essentially reduced into a one-dimensional problem. The governing equation of the duct field is[15]

$$\frac{1}{c^2}\frac{\partial^2 p(x,t)}{\partial t^2}-\frac{\partial^2 p(x,t)}{\partial x^2}=f(x,t), \tag{1}$$

subject to the boundary conditions

$$\frac{\partial p(0,t)}{\partial x}=-\rho\frac{\partial v(0,t)}{\partial t}=-\rho a(0,t), \tag{2}$$

$$p(l,t)=z_n v(l,t), \tag{3}$$

and some initial conditions, where $p(x,t)$ is the sound pressure in the duct, $a(0,t)$ is the surface acceleration of the piston, $f(x,t)$ is the control function, c is the speed of sound, and ρ is the density of medium. The open end of the duct can be approximated by a pressure-released boundary with the effective length of the duct L increased by $0.6\times$ the radius a (for an unflanged circular duct).[15] That is,

$$p(x,t)=0 \quad \text{at } x=L(=l+0.6a). \tag{4}$$

Solving the eigenvalue problem associated with Eqs. (1), (2), and (4) yields the eigenvalues

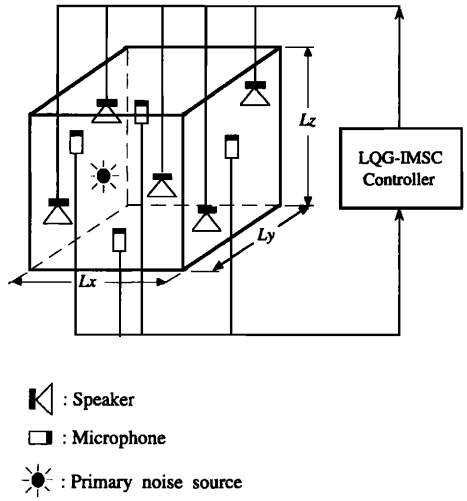

FIG. 2. Configuration of the LQG-IMSC system for a 1 m×1.5 m×2 m rectangular room containing a monopole noise source.

$$\lambda_r=[(\pi/2L)(2r-1)]^2, \quad r=1,2,\ldots,\infty \tag{5}$$

and the normalized eigenfunctions

$$\phi_r(x)=c\sqrt{2/L}\cos\sqrt{\lambda_r}x. \tag{6}$$

Since the orthogonal eigenfunctions $\phi_r(x)$ form a complete set, the sound pressure $p(x,t)$ and the control function $f(x,t)$ can be expanded as follows:

$$p(x,t)=\sum_{r=1}^{\infty} p_r(t)\phi_r(x), \tag{7}$$

$$f(x,t)=\sum_{r=1}^{\infty}\frac{1}{c^2}f_r(t)\phi_r(x), \tag{8}$$

where $p_r(t)$ is the modal pressure and $f_r(t)$ is the modal control function. Conversely, $p_r(t)$ and $f_r(t)$ can be extracted by *modal filtering*:[16]

$$p_r(t)=\int_0^L\frac{1}{c^2}p(x,t)\phi_r(x)dx, \tag{9}$$

$$f_r(t)=\int_0^L f(x,t)\phi_r(x)dx. \tag{10}$$

With some manipulations, the modal equation for the duct can thus be expressed as[16]

$$\frac{d^2p_r(t)}{d^2t}+\lambda_r c^2 p_r(t)=\sqrt{\frac{2}{L}}\rho c^2 a(t)+f_r(t), \quad r=1,2,\ldots,\infty, \tag{11}$$

where the first term at the right-hand side represents the modal excitation due to the primary noise.

On the other hand, assume that a rectangular room of dimensions L_x, L_y, and L_z, as shown in Fig. 2, is bounded by rigid walls. A monopole source with known volume velocity per unit volume $q(t)$ is present in the room. Hence the governing equation of the problem is

Redistribution subject to ASA license or copyright; see http://acousticalsociety.org/content/terms. Download to IP: 140.113.38.11 On: Wed, 30 Apr 2014 06:45:39

$$\frac{1}{c^2}\frac{\partial^2 p(\mathbf{x},t)}{\partial t^2}=\nabla^2 p(\mathbf{x},t)+\rho\frac{\partial}{\partial t}q(t)\delta(\mathbf{x}-\mathbf{x}_s)+f(\mathbf{x},t), \tag{12}$$

subject to the rigid-walled boundary conditions

$$\begin{aligned}&\frac{\partial p}{\partial x}(0,y,z,t)=0, \quad \frac{\partial p}{\partial x}(L_x,y,z,t)=0,\\ &\frac{\partial p}{\partial y}(x,0,z,t)=0, \quad \frac{\partial p}{\partial y}(x,L_y,z,t)=0,\\ &\frac{\partial p}{\partial z}(x,y,0,t)=0, \quad \frac{\partial p}{\partial z}(x,y,L_z,t)=0,\end{aligned} \tag{13}$$

and some initial conditions, where $\mathbf{x}=(x,y,z)$ and $\mathbf{x}_s=(x_s,y_s,z_s)$ are the position vectors of the field point and the source point, respectively, $f(\mathbf{x},t)$ is the control function, and $\delta(\mathbf{x}-\mathbf{x}_s)$ is the three-dimensional Dirac delta function. Solving the eigenvalue problem of Eqs. (12) and (13) yields the eigenvalues

$$\lambda_r=\left(\frac{n_x\pi}{L_x}\right)^2+\left(\frac{n_y\pi}{L_y}\right)^2+\left(\frac{n_z\pi}{L_z}\right)^2 \tag{14}$$

and the normalized eigenfunctions

$$\phi_r(\mathbf{x})=c\sqrt{\frac{8}{L_xL_yL_z}}\cos\left(\frac{n_x\pi x}{L_x}\right)\cos\left(\frac{n_y\pi y}{L_y}\right)\cos\left(\frac{n_z\pi z}{L_z}\right), \tag{15}$$

where $n_x,n_y,n_z=0,1,2,\ldots,\infty$ and $r=1,2,\ldots,\infty$. Note that the subscript r is being used as a triple index, so that $r=(n_x,n_y,n_z)$. Then, similar to the duct case, the sound pressure $p(\mathbf{x},t)$ and the control function $f(\mathbf{x},t)$ can be expanded on the basis of the eigenfunctions

$$p(\mathbf{x},t)=\sum_{r=1}^{\infty}p_r(t)\phi_r(\mathbf{x}), \tag{16}$$

$$f(\mathbf{x},t)=\sum_{r=1}^{\infty}1/c^2 f_r(t)\phi_r(\mathbf{x}). \tag{17}$$

Using the orthogonality of eigenfunctions, the modal pressure and the modal control function can be obtained by the modal filter

$$p_r(t)=\int_V\frac{1}{c^2}p(\mathbf{x},t)\phi_r(\mathbf{x})d\mathbf{x}, \tag{18}$$

$$f_r(t)=\int_V f(\mathbf{x},t)\phi_r(\mathbf{x})d\mathbf{x}, \tag{19}$$

where V is the domain of the volume integral for the room. Thus the partial differential equation in Eq. (12) can be uncoupled into the following modal equations:[16]

$$\frac{d^2p_r(t)}{dt^2}+\lambda_r c^2 p_r(t)=\rho\frac{\partial}{\partial t}q(t)\phi_r(\mathbf{x}_s)+f_r(t), \quad r=1,2,\ldots,\infty. \tag{20}$$

It can be observed from Eqs. (11) and (20) that the modal equations of the one-dimensional duct problem and the three-dimensional room problem are essentially of the same form except for the definitions of the eigenfunctions and the source terms.

B. Control by state feedback and estimation

Continuous systems such as the aforementioned duct and room have an infinite number of natural modes. This requires an infinite-order controller if global control is desired. In practice, modal truncation is often necessary to include only the predominant low-order modes (say, n modes) in order for the controller to be implementable. This leads to a finite number of modal equations

$$\frac{d^2p_r(t)}{d^2t}+\lambda_r c^2 p_r(t)=\sqrt{\frac{2}{L}}\rho c^2 a(t)+f_r(t), \quad r=1,2,\ldots,n \tag{21}$$

for the duct and

$$\frac{d^2p_r(t)}{dt^2}+\lambda_r c^2 p_r(t)=\rho\frac{\partial}{\partial t}q(t)\phi_r(\mathbf{x}_s)+f_r(t), \quad r=1,2,\ldots,n \tag{22}$$

for the rectangular room. Either of the modal equations in Eqs. (21) and (22) can be expressed as the following modal state form (for the rth mode only):

$$\begin{aligned}\dot{\mathbf{x}}_r(t)&=\mathbf{A}_r\mathbf{x}_r(t)+\mathbf{B}_r f_r(t)+\mathbf{w}_{r1}(t),\\ y_r(t)&=\mathbf{C}_r\mathbf{x}_r(t)+\mathbf{D}_r\mathbf{w}_{r2}(t),\end{aligned} \tag{23}$$

where $\mathbf{x}_r=[\omega_r p_r(t)\dot{p}_r(t)]^T$ is the rth modal state vector, $\omega_r=c\sqrt{\lambda_r}$ is the rth nature frequency, $f_r(t)$ is the modal control function for the loudspeakers, and $y_r(t)$ is the modal output measured by the microphones. Note that the first component of the state vector is given as $\omega_r p_r(t)$, rather than just $p_r(t)$ for better conditioning of matrices. This is a necessary step to avoid numerical problems in solving the Riccatti equation. The coefficient matrices in the modal state equation are accordingly defined as

$$\mathbf{A}_r=\begin{bmatrix}0 & \omega_r\\ -\omega_r & 0\end{bmatrix}, \quad \mathbf{B}_r=\begin{bmatrix}0\\ 1\end{bmatrix}, \quad \mathbf{C}_r=[1/\omega_r \quad 0], \quad \mathbf{D}_r=[0 \quad 1]. \tag{24}$$

The matrices $\mathbf{w}_{r1}(t)$ and $\mathbf{w}_{r2}(t)$ representing the noise terms of the source and the sensor, respectively, in the modal space are defined as

$$\mathbf{w}_{r1}(t)=\begin{bmatrix}0\\ \sqrt{2/L}\rho c^2 a(t)\end{bmatrix} \text{ for the duct or} \tag{25}$$

$$\mathbf{w}_{r1}(t)=\begin{bmatrix}0\\ \rho\dfrac{\partial}{\partial t}q(t)\phi_r(\mathbf{x}_s)\end{bmatrix} \text{ for the room and} \tag{26}$$

$$\mathbf{w}_{r2}(t)=\begin{bmatrix}0\\ W_{r2}(t)\end{bmatrix} \text{ for both the duct and the room,} \tag{27}$$

where $W_{r2}(t)$ is the intensity of the modal sensor noise. It can be proved that the modal state equations are both *con-*

Redistribution subject to ASA license or copyright; see http://acousticalsociety.org/content/terms. Download to IP: 140.113.38.11 On: Wed, 30 Apr 2014 06:45:39

trollable and *observable*.[5] In the study, the source noise and the sensor noise are assumed to be zero mean and Gaussian white. That is, the covariance matrix of the noise terms satisfies

$$E\left\{\begin{bmatrix}\mathbf{W}_{r1}(t_1)\\ \mathbf{W}_{r2}(t_1)\end{bmatrix}[\mathbf{W}_{r1}^T(t_2) \quad \mathbf{W}_{r2}^T(t_2)]\right\}=\mathbf{V}_r(t_1)\,\delta(t_1-t_2), \tag{28}$$

where the intensity matrix of the joint process $\mathbf{V}_r(t)$ is defined as

$$\mathbf{V}_r(t)=\begin{bmatrix}\mathbf{V}_{r11}(t) & \mathbf{V}_{r12}(t)\\ \mathbf{V}_{r21}^T(t) & \mathbf{V}_{r22}(t)\end{bmatrix}, \tag{29}$$

with

$$\mathbf{V}_{r11}=\begin{bmatrix}0 & 0\\ 0 & V_{r11}\end{bmatrix}, \quad \mathbf{V}_{r12}=\mathbf{V}_{r21}=\begin{bmatrix}0 & 0\\ 0 & V_{r12}\end{bmatrix},$$

$$\mathbf{V}_{r22}=\begin{bmatrix}0 & 0\\ 0 & V_{r22}\end{bmatrix}.$$

Here, the stochastic process is said to be *nonsingular* if $V_{r22}>0$ and *uncorrelated* if $V_{r12}=0$.[3] In our case, we restricted ourselves to the controller design for the nonsingular and uncorrelated white noise only.

According to the method of IMSC, state feedback is carried out for each individual mode of the physical plant. Hence the modal control function of the rth mode is generated as a linear combination of the modal pressure and its first time derivative, i.e.,

$$f_r(t)=\mathbf{G}_r\mathbf{x}_r=-g_r p_r(t)-h_r\dot{p}_r(t). \tag{30}$$

One question remaining is how to determine the modal gains g_r and h_r in Eq. (30). Two of the commonly used techniques are pole allocation and optimal control.[12–14] In this research, the latter method is adopted because it not only admits a reasonable balance between the control error and control energy but also yields a stable control system. Since the acoustic system in our case is subjected to stochastic excitations, a more general optimal control approach, the LQG algorithm, is employed.[3,14] Note, however, that the presence of the Gaussian white noise in the system does not alter the form of solution as its deterministic LQ version, except to increase the minimal value of the optimal criterion.[3] Because modal coupling is neglected, the global optimum can be obtained by minimizing the following performance index for individual modes:

$$J_r=E\left\{\int_{t_0}^{t_1}(\mathbf{x}_r^T\mathbf{Q}_r\mathbf{x}_r+R_r f_r^2)dt+\mathbf{x}_r^T\mathbf{P}_{1r}\mathbf{x}_r\right\}, \tag{31}$$

where $E\{\ \}$ denotes the expected value, $\mathbf{Q}_r=\mathrm{diag}\{Q_r,Q_r\}$, $Q_r\geqslant 0$, $R_r>0$, $\mathbf{P}_{1r}$ is a real symmetric positive semidefinite matrix, and t_0 and t_1 are the initial time and the final time, respectively. The scalars Q_r and R_r stipulate the relative importance of the control error and control energy. A large $Q_r:R_r$ ratio corresponds to *expensive* control, while a small $Q_r:R_r$ ratio corresponds to *cheap* control. Minimization of the performance index in Eq. (31) amounts to regulating the system response as close to the zero state while, on the other hand, keeping the expenditure of control energy as low as possible.

The optimal modal control gains g_r and h_r in accord with the performance index in Eq. (31) can be calculated by

$$\mathbf{G}_r=R_r^{-1}\mathbf{B}_r^T\mathbf{P}_r, \tag{32}$$

where $\mathbf{P}_r$ is the solution of the Riccati equation[3]

$$-\dot{\mathbf{P}}_r=R_r\mathbf{I}-\mathbf{P}_r\mathbf{B}_r^T R_r^{-1}\mathbf{B}_r\mathbf{P}_r+\mathbf{A}_r^T\mathbf{P}_r+\mathbf{P}_r\mathbf{A}_r, \tag{33}$$

subject to the final condition $\mathbf{P}_{1r}(t_1)=\mathbf{P}_{1r}$, where $\mathbf{I}$ is a 2×2 identity matrix. In this study, only the steady-state case is of concern, i.e., $\dot{\mathbf{p}}_r=0$, and Eq. (33) reduces to the algebraic Riccati equation. Solving the algebraic Riccati equation leads to the following closed-form solutions:

$$\begin{aligned}
p_{r11}&=R_r\{2\omega_r[\sqrt{\omega_r^2+(\omega_r^2+R_r)^{-1}R_r}-\omega_r]\}^{1/2},\\
p_{r12}&=p_{r21}=R_r[\sqrt{\omega_r^2+(\omega_r^2+R_r)^{-1}R_r}-\omega_r],\\
p_{r22}&=R_r\{-2[\omega_r^2+(\omega_r^2R_r)^{-1}R_r]\\
&\quad+2\omega_r^{-1}[\omega_r^2+(\omega_r^2R_r)^{-1}R_r]^{3/2}\}^{1/2}.
\end{aligned} \tag{34}$$

The modal LQG regulator should work very well when the information of states is fully available. In reality, however, the information of states is generally incomplete or inaccurate. This calls for the need of a modal state observer that is based on the Kalman–Bucy filter[3]

$$\dot{\hat{\mathbf{x}}}_r(t)=\mathbf{A}_r\hat{\mathbf{x}}_r(t)+\mathbf{B}_r f_r+\mathbf{K}_r[y_r(t)-\mathbf{C}_r\hat{\mathbf{x}}_r(t)], \tag{35}$$

where $\hat{\mathbf{x}}_r(t)=[\omega_r\hat{p}_r(t) \quad \dot{\hat{p}}_r(t)]^T$ is the estimated modal state vector. Consider the state estimation error

$$\mathbf{e}_r(t)=\hat{\mathbf{x}}_r(t)-\mathbf{x}_r(t). \tag{36}$$

The optimization problem amounts to finding the modal gain matrix $\mathbf{K}_r$ such that the weighted mean-square estimation error $E\{\mathbf{e}_r^T(t)\mathbf{W}_r\mathbf{e}_r(t)\}$ is minimized, where $\mathbf{W}_r$ is a symmetric and positive definite matrix. The optimal solution of the matrix $\mathbf{K}_r$ (which is independent of the matrix $\mathbf{W}_r$) can be calculated by[3]

$$\mathbf{K}_r(t)=\mathbf{Q}_r(t)\mathbf{C}_r^T(t)V_{r22}^{-1}(t), \quad t\geqslant t_0, \tag{37}$$

where Q_r is the solution of the Riccati equation

$$\dot{\mathbf{Q}}_r=V_{r11}\mathbf{I}-\mathbf{Q}_r\mathbf{C}_r^T V_{r22}^{-1}\mathbf{C}_r\mathbf{Q}_r+\mathbf{Q}_r\mathbf{A}_r^T+\mathbf{A}_r\mathbf{Q}_r. \tag{38}$$

Since only the steady-state case is of interest ($\dot{\mathbf{Q}}_r=0$), the closed-form solution of $\mathbf{Q}_r$ simply reads

$$\begin{aligned}
Q_{r11}&=V_{r11}\{2\omega_r[\sqrt{\omega_r^2+(\omega_r^2+V_{r11})^{-1}V_{r11}}-\omega_r]\}^{1/2},\\
Q_{r12}&=V_{r11}[\sqrt{\omega_r^2+(\omega_r^2+V_{r11})^{-1}V_{r11}}-\omega_r],\\
Q_{r22}&=V_{r11}\{-2[\omega_r^2+(\omega_r^2V_{r11})^{-1}V_{r11}]\\
&\quad+2\omega_r^{-1}[\omega_r^2+(\omega_r^2V_{r11})^{-1}V_{r11}]^{3/2}\}^{1/2}.
\end{aligned} \tag{39}$$

Redistribution subject to ASA license or copyright; see http://acousticalsociety.org/content/terms. Download to IP: 140.113.38.11 On: Wed, 30 Apr 2014 06:45:39

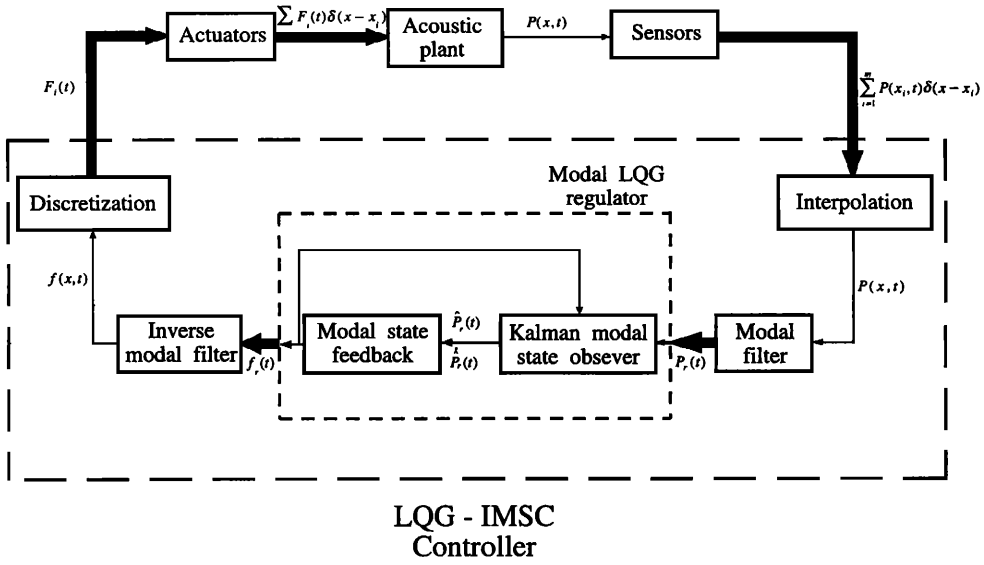

FIG. 3. Overall ANC system framework based on the LQG-IMSC technique.

C. Discrete sensors and actuators

The ideal IMSC formulation requires distributed sensors and actuators. If this requirement is satisfied, then every mode of the continuous system can be controlled and no spillover will occur.[5] In practical implementation of the ANC system, only discrete loudspeakers and microphones are available from the state of art. This produces spillover problems, as will be discussed in the end of this section.

First, the numerical aspect concerned with discrete sensors is discussed. Since in practice sound pressure can only be measured by a finite number of discrete microphones, an appropriate interpolation scheme must be used to accurately reconstruct the original acoustic field, i.e.,

$$\hat{p}(\mathbf{x},t)=\sum_{i=1}^{m} S_i(\mathbf{x})p(\mathbf{x}_i,t), \tag{40}$$

where $\hat{p}(\mathbf{x},t)$ is the interpolated sound pressure, $p(\mathbf{x}_i,t)$ are the sound pressures measured by the finite number of discrete microphones, and $S_i(\mathbf{x})$ are interpolation functions. Several options of interpolation functions are available.[17] In this study, the interpolation function based on the Rayleigh–Ritz method is employed to reconstruct the acoustic field because it makes use of the eigenfunctions that provide a better approximation of the system characteristics. According to the Rayleigh–Ritz method, the sound pressure $p(\mathbf{x},t)$ can be expressed as the linear combination of eigenfunctions $\phi_r(\mathbf{x})$:

$$p(\mathbf{x},t)=\sum_{r=1}^{n} a_r(t)\phi_r(\mathbf{x}), \tag{41}$$

where $a_r(t)$ are the modal coordinates. Therefore substituting m measured sound-pressure data $\{p(\mathbf{x}_i,t)\}$, $i=1,2,\ldots,m$ into Eq. (41) gives the following linear equations:

$$\begin{Bmatrix} p(\mathbf{x}_1,t) \\ p(\mathbf{x}_2,t) \\ \cdot \\ \cdot \\ \cdot \\ p(\mathbf{x}_m,t) \end{Bmatrix} = \begin{bmatrix} \phi_1(\mathbf{x}_1) & \phi_2(\mathbf{x}_1) & \cdots & \phi_n(\mathbf{x}_1) \\ \phi_1(\mathbf{x}_2) & \phi_2(\mathbf{x}_2) & \cdots & \phi_n(\mathbf{x}_2) \\ \cdot & \cdot & \cdots & \cdot \\ \cdot & \cdot & \cdots & \cdot \\ \cdot & \cdot & \cdots & \cdot \\ \phi_1(\mathbf{x}_m) & \phi_2(\mathbf{x}_m) & \cdots & \phi_n(\mathbf{x}_m) \end{bmatrix} \times \begin{Bmatrix} a_1(t) \\ a_2(t) \\ \cdot \\ \cdot \\ \cdot \\ a_n(t) \end{Bmatrix}, \tag{42}$$

or, written more compactly,

$$\{p(\mathbf{x}_i,t)\}=[\Phi]\{a_r(t)\}, \tag{43}$$

where $[\Phi]$ is an $m\times n$ real matrix that contains spatially sampled eigenfunctions. The coefficients $\{a_r(t)\}$ can be obtained by pseudoinverting Eq. (43):

$$\{a_r(t)\}=[\Phi]^{+}\{p(\mathbf{x}_i,t)\}. \tag{44}$$

Note that the pseudoinverse becomes the actual inverse for a nonsingular $[\Phi]$ if the same number of microphones is used as the controlled modes. Substituting Eq. (44) into Eq. (41) yields

$$p(\mathbf{x},t)=\sum_{i=1}^{m}\sum_{r=1}^{n} [\Phi]_{ri}^{+}\phi_r(\mathbf{x})p(\mathbf{x}_i,t), \tag{45}$$

where $[\Phi]_{ri}^{+}$ stands for the ri component of the matrix $[\Phi]^{+}$. Comparing Eq. (45) with Eq. (40) indicates that the interpolation function based on the Rayleigh–Ritz method takes the following form:

Redistribution subject to ASA license or copyright; see http://acousticalsociety.org/content/terms. Download to IP: 140.113.38.11 On: Wed, 30 Apr 2014 06:45:39

TABLE I. Simulation cases for the duct.

Case	Controlled modes	Noise type	Sensor location	Actuator location	Number of transducers	Q:R ratio
1	first 4	white noise	arbitrary	arbitrary	4	100:1
2	first 2	white noise	arbitrary	arbitrary	4	100:1
3	first 4	white noise	arbitrary	arbitrary	2	100:1
4	first 4	white noise	arbitrary	at nodal point 4	4	100:1
5	first 4	white noise	at nodal point 4	arbitrary	4	100:1
6	first 4	white noise	at nodal point 4	at nodal point 4	4	100:1
7	first 4	white noise	arbitrary	arbitrary	4	1000:1
8	first 4	sinusoid	arbitrary	arbitrary	4	100:1

$$S_i(\mathbf{x})=\sum_{r=1}^{n}[\Phi]_{ri}^{+}\phi_r(\mathbf{x}). \tag{46}$$

Parallel to the above-mentioned discrete sensor problem, a finite number of discrete loudspeakers employed to control the acoustic fields renders a similar approximation problem. If one uses as many loudspeakers as microphones and allocates the loudspeakers at the points $\mathbf{x}_i$, $i=1,2,\ldots,m$, the associated control function can be written as

$$f(\mathbf{x},t)=\sum_{i=1}^{m}F_i(t)\,\delta(\mathbf{x}-\mathbf{x}_i), \tag{47}$$

where $F_i(t)$ are the amplitudes of the discrete control functions produced by the ith loudspeaker. This corresponds to the modal control functions

$$f_r(t)=\sum_{i=1}^{m}\phi_r(\mathbf{x}_i)F_i(t), \quad r=1,2,\ldots,n, \tag{48}$$

which can also be written in the following matrix form:

$$\{f_r(t)\}=[\Phi]\{F_i(t)\}, \tag{49}$$

where $[\Phi]$ has the same form as in Eq. (43). In IMSC, the modal control functions are determined first and the actual control functions are then computed. Hence we need the inverse relation to that given by Eq. (49), i.e.,

$$\{F_i(t)\}=[\Phi]^{+}\{f_r(t)\}, \tag{50}$$

where $[\Phi]^{+}$ is the pseudoinverse of $[\Phi]$. It should be noted that a pseudoinverse is not an actual inverse and the above process does not yield genuine IMSC. To design a control function for each controlled mode independently as required by IMSC, one must have as many loudspeakers and microphones as the controlled modes, $m=n$, in which case $[\Phi]^{+}=[\Phi]^{-1}$. The effect of this point will be explored further in Sec. II.

A final note regarding spillover effects is in order. It can be shown in IMSC that control spillover will not destabilize the system, although it can cause degradation in the system performance.[5] Observation spillover alters the system eigenvalues and can possibly produce instability in the residual modes. This is particularly true if the loudspeakers and microphones are not collocated.[5]

The overall ANC system framework based on the LQG-IMSC technique is depicted in Fig. 3. The sound pressure measured by the discrete microphones is interpolated, modal filtered, and fed to the modal LQG regulator. The regulator then produces optimal modal control functions that are in turn sent to the inverse modal filter and discretized into ac-

TABLE II. Simulation cases for the rectangular room.

Case	Controlled modes	Sensor location	Actuator location	Number of transducers	Q:R ratio
1	first 4	arbitrary	arbitrary	4	100:1
2	first 2	arbitrary	arbitrary	4	100:1
3	first 4	arbitrary	arbitrary	2	100:1
4	first 4	arbitrary	at nodal plane (0,1,1)	4	100:1
5	first 4	at nodal plane (0,1,1)	arbitrary	4	100:1
6	first 4	at nodal plane (0,1,1)	at nodal plane (0,1,1)	4	100:1

Redistribution subject to ASA license or copyright; see http://acousticalsociety.org/content/terms. Download to IP: 140.113.38.11 On: Wed, 30 Apr 2014 06:45:39

TABLE III. Modal frequencies of the acoustic field inside the duct.

Mode index	Modal frequency (Hz)
1	43.1
2	129.4
3	215.7
4	302.0
5	388.3
6	474.6
7	560.9
8	647.2

tual control functions for the discrete loudspeakers. The entire process forms a closed-loop modal control system for noise cancellation.

II. NUMERICAL SIMULATION

Simulation cases are designed to investigate the effects of control parameters on the LQG-IMSC technique. The parameters for the simulation include the type of primary noise, number of controlled modes, number of sensors and actuators, location of sensors and actuators, and the Q:R ratio. The simulation cases for the duct and the room are shown in Tables I and II, respectively. Although mode shapes are global properties and the modal control technique should presumably achieve global control, the results presented below show the power spectra (in decibels) calculated by averaging the sound pressure only at the sensor locations. This is not only because of the limitation of computer facility but also because we are more interested in creating quiet zones, e.g., the vicinity of the passenger's heads in a car cabin, which is in fact the only possibility in practical applications at high-frequency ranges.[2] The power spectrum calculation is based on 20 records of 1024 time samples for FFT. In each of the following cases, the simulation parameters will be changed one at a time to investigate the performance of the LQG-IMSC controller.

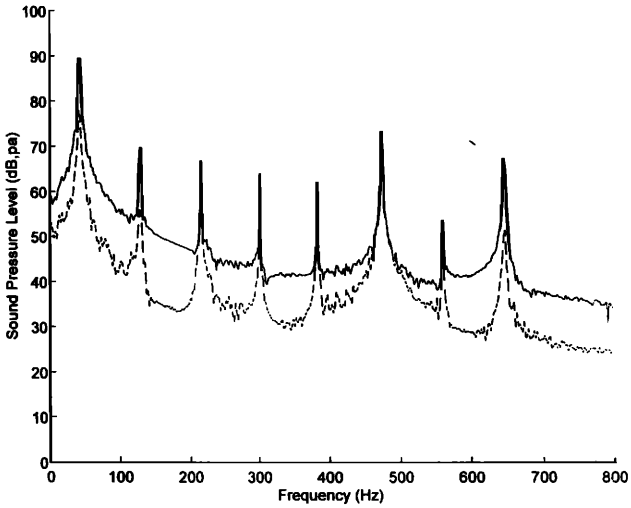

FIG. 5. Response spectrum of case 2 for the duct problem (——— uncontrolled field; --- controlled field). Four microphones and four loudspeakers are employed to control the first two modes. The microphones and loudspeakers are collocated at x=0.25, 0.75, 1.25, and 1.75 m, respectively. The Q:R ratio is selected to be 100:1.

A. The duct case

The LQG-IMSC technique is first applied to a duct of length 2 m and radius 0.1 m whose natural frequencies associated with the first eight acoustic modes are listed in Table III. In case 1, four loudspeakers and four microphones are used to control the first four modes with Q:R=100:1. The primary noise is zero-mean Gaussian white noise. This is chosen as the reference case. In the simulation result of Fig. 4, significant reduction (maximum 20 dB) of the sound-pressure spectrum can be observed in the frequency range of interest (800 Hz). It is interesting to note that all of the first eight modes are affected by not only the control action (for the first four modes) but also the spillover effect.

In case 2, the controller performance is investigated if

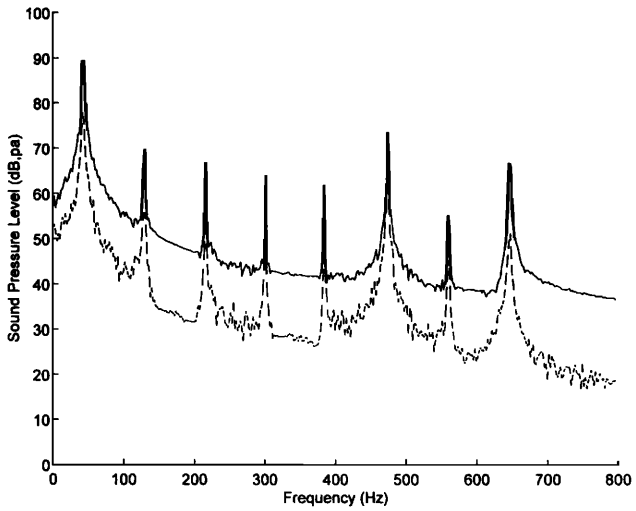

FIG. 4. Response spectrum of case 1 for the duct problem (——— uncontrolled field; --- controlled field). Four microphones and four loudspeakers are employed to control the first four modes. The microphones and loudspeakers are collocated at x=0.25, 0.75, 1.25, and 1.75 m, respectively. The Q:R ratio is selected to be 100:1.

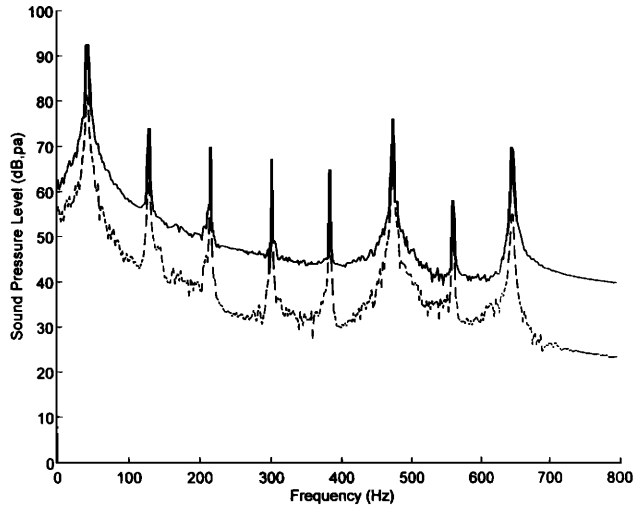

FIG. 6. Response spectrum of case 3 for the duct problem (——— uncontrolled field; --- controlled field). Two microphones and two loudspeakers are employed to control the first four modes. The microphones and loudspeakers are collocated at x=0.25, 0.75, 1.25, and 1.75 m, respectively. The Q:R ratio is selected to be 100:1.

Redistribution subject to ASA license or copyright; see http://acousticalsociety.org/content/terms. Download to IP: 140.113.38.11 On: Wed, 30 Apr 2014 06:45:39

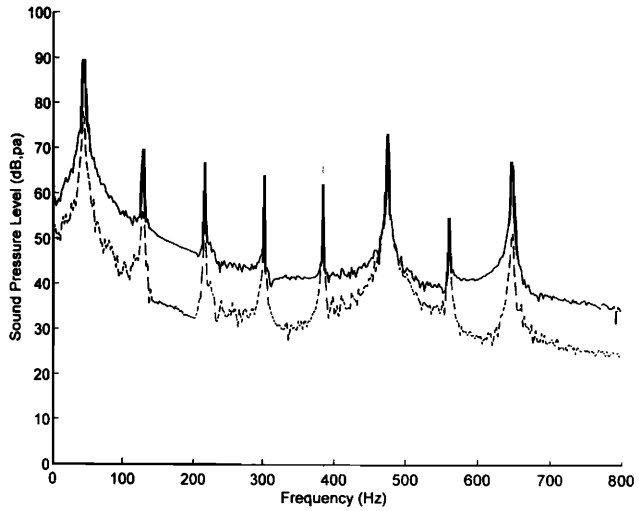

FIG. 7. Response spectrum of case 4 for the duct problem (——— uncontrolled field; --- controlled field). Four microphones and four loudspeakers are employed to control the first four modes. The microphones are located at $x=0.25$, 0.75, 1.25, and 1.75 m, respectively. The loudspeakers are collocated at $x=0.86$ m, which is the nodal point of the fourth mode. The Q:R ratio is selected to be 100:1.

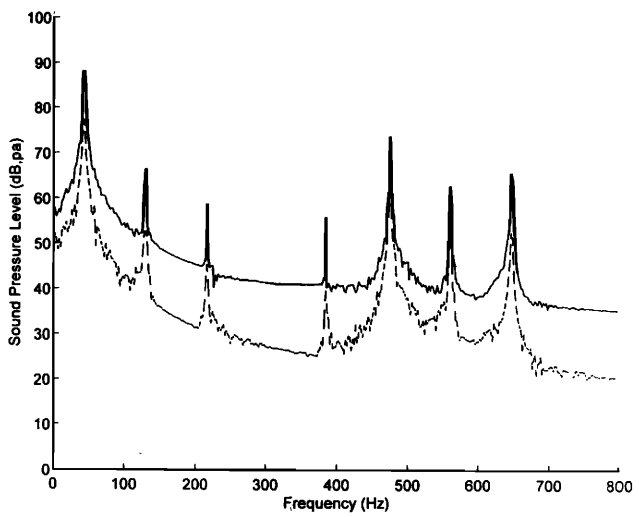

FIG. 9. Response spectrum of case 6 for the duct problem (——— uncontrolled field; --- controlled field). Four microphones and four loudspeakers are employed to control the first four modes. The microphones and loudspeakers are collocated at $x=0.86$ m, which is the nodal point of the fourth mode. The Q:R ratio is selected to be 100:1.

only the first two modes are controlled. As shown in Fig. 5, excellent noise reduction of the first two modes is obtained, while the third mode and the fourth mode remain unchanged. The peaks of the seventh mode and the eighth mode are changed due to spillover effects.

In case 3, the number of microphones and loudspeakers is reduced to two. The simulation result is shown in Fig. 6. Comparison between the results of cases 3 and 1 suggests that satisfactory performance of the controller can be achieved if a large number of transducers are used. This not unexpected since a large number of microphones and loudspeakers provide better approximations to the distributed field as required by the IMSC formulation.

Because the loudspeakers and microphones are of discrete nature, how one places these transducers is critical to the controller performance. In case 4, the effect of locations of loudspeakers is investigated. If loudspeakers are placed at the nodal point of the fourth mode, the result in Fig. 7 shows that the peak of the fourth mode has not been reduced. The fourth mode is uncontrollable by this loudspeaker arrangement. Conversely, in case 5, if the microphones are placed at the nodal point of the fourth mode, the result in Fig. 8 shows that no attenuation has occurred at the peak of the fourth mode. The fourth mode is unobservable by this microphone arrangement. In case 6, the microphones and loudspeakers are collocated at the nodal point of the fourth mode. It can be observed from the result in Fig. 9 that the performance is improved.

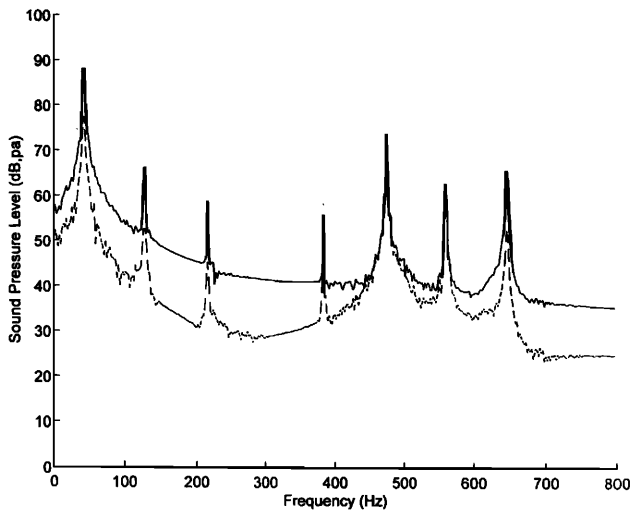

FIG. 8. Response spectrum of case 5 for the duct problem (——— uncontrolled field; --- controlled field). Four microphones and four loudspeakers are employed to control the first four modes. The microphones are collocated at $x=0.86$ m, which is the nodal point of the fourth mode. The loudspeakers are located at $x=0.25$, 0.75, 1.25, and 1.75 m, respectively. The Q:R ratio is selected to be 100:1.

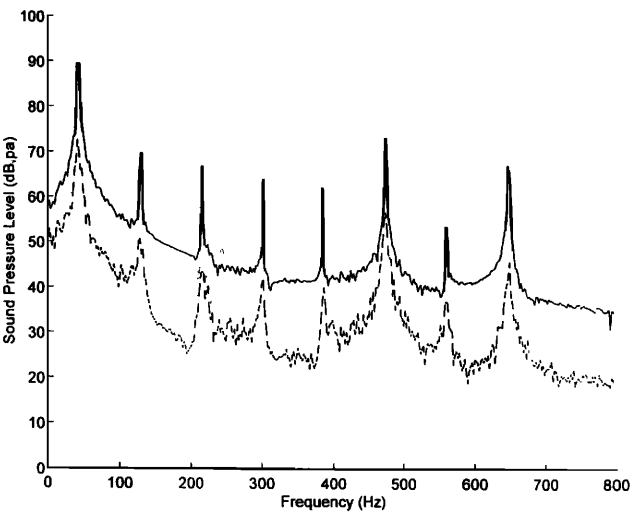

FIG. 10. Response spectrum of case 7 for the duct problem (——— uncontrolled field; --- controlled field). Four microphones and four loudspeakers are employed to control the first four modes. The microphones and loudspeakers are collocated at $x=0.25$, 0.75, 1.25, and 1.75 m, respectively. The Q:R ratio is selected to be 1000:1.

Redistribution subject to ASA license or copyright; see http://acousticalsociety.org/content/terms. Download to IP: 140.113.38.11 On: Wed, 30 Apr 2014 06:45:39

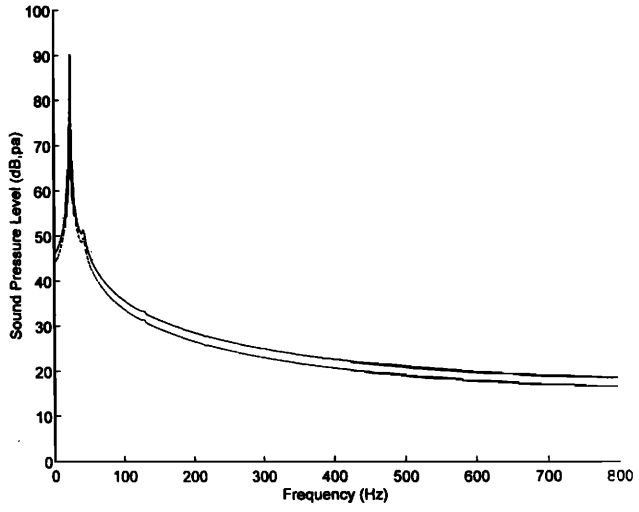

FIG. 11. Response spectrum of case 8 for the duct problem (——— uncontrolled field; --- controlled field). Four microphones and four loudspeakers are employed to control the first four modes. The microphones and loudspeakers are collocated at $x=0.25$, 0.75, 1.25, and 1.75 m, respectively. The Q:R ratio is selected to be 100:1. The primary noise is the sinusoidal signal.

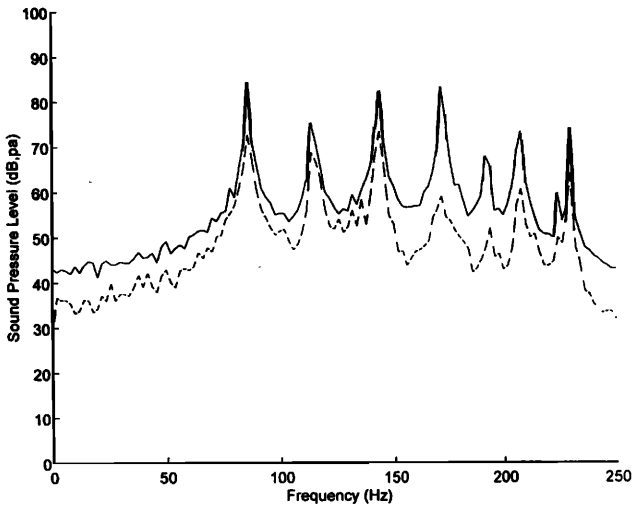

FIG. 12. Response spectrum of case 1 for the rectangular room problem (——— uncontrolled field; --- controlled field). Four microphones and four loudspeakers are employed to control the first four modes. The microphones and loudspeakers are collocated at (0.1, 0.2, 0.3), (0.2, 0.7, 1.3), (0.15, 1.3, 1.6), and (0.9, 1.4, 1.9 m), respectively. The Q:R ratio is selected to be 100:1.

In case 7, the Q:R ratio is further increased to 1000:1, while the other settings remain the same as in case 1. The result in Fig. 10 shows that larger reduction of noise level can indeed be obtained than that of case 1. However, one may not be able to increase the Q:R ratio indefinitely in practical implementation since this may overdrive the loudspeakers.

As can be seen in the above-mentioned cases, Gaussian white noises can be successfully suppressed by the LQG-IMSC technique. In case 8, the primary noise is changed into sinusoidal type. The result in Fig. 11 shows that the LQG algorithm yields only limited attenuation away from the frequency of the sinusoid but no attenuation at the frequency of the sinusoid. This is because the sinusoidal noise is non-Gaussian type and thus the Kalman–Bucy filter does not function properly. More precisely, the solution of the Riccatti equation based on the assumption of Gaussian noise is no longer the optimal one for the sinusoid. This implies that, for the highly correlated non-Gaussian noises, such as the sinusoids and periodic noises, one should resort to simpler methods like repetitive control.[18]

B. The rectangular room case

Next, the LQG-IMSC technique is applied to a rectangular room of dimensions 1 m×1.5 m×2 m whose natural frequencies associated with the first eight acoustic modes are listed in Table IV. Several important parameters explored in the duct case, such as number of controlled modes, number of microphones and loudspeakers, and location of sensors and loudspeakers, will be revisited for the rectangular room case.

TABLE IV. Modal frequencies of the acoustic field inside the rectangular room.

Mode index	Modal frequency (Hz)
(0,0,1)	86.3
(0,1,0)	115.0
(0,1,1)	143.8
(1,0,0) and (0,0,2)	172.6
(1,0,1)	193.0
(1,1,0) and (0,1,2)	207.4
(1,1,1)	224.7
(0,2,0)	230.1

In case 1, four loudspeakers and four microphones are used to control the first four modes of the sound field inside the rectangular room. This is used as the reference case. The simulation result in Fig. 12 shows significant noise reduction of all modes (maximum 30 dB) achieved by the LQG-IMSC technique. If four actuators are used, four modes can be controlled independently. Although more modes can be attenuated than expected, as demonstrated in Fig. 12, it is actually

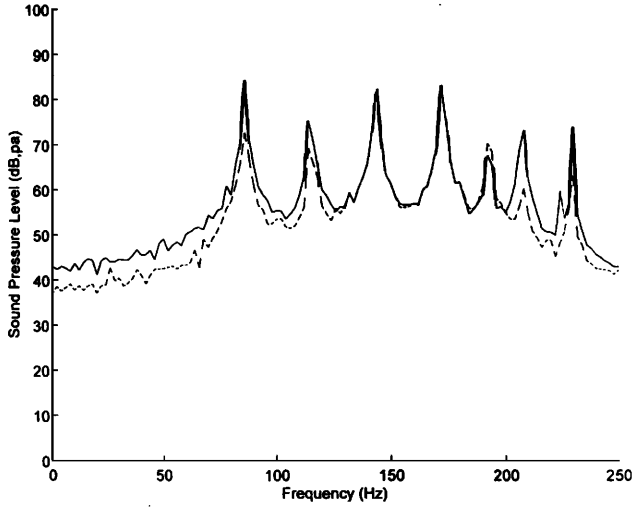

FIG. 13. Response spectrum of case 2 for the rectangular room problem (——— uncontrolled field; --- controlled field). Four microphones and four loudspeakers are employed to control the first two modes. The microphones and loudspeakers are collocated at (0.1, 0.2, 0.3), (0.2, 0.7, 1.3), (0.15, 1.3, 1.6), and (0.9, 1.4, 1.9 m), respectively. The Q:R ratio is selected to be 100:1.

Redistribution subject to ASA license or copyright; see http://acousticalsociety.org/content/terms. Download to IP: 140.113.38.11 On: Wed, 30 Apr 2014 06:45:39

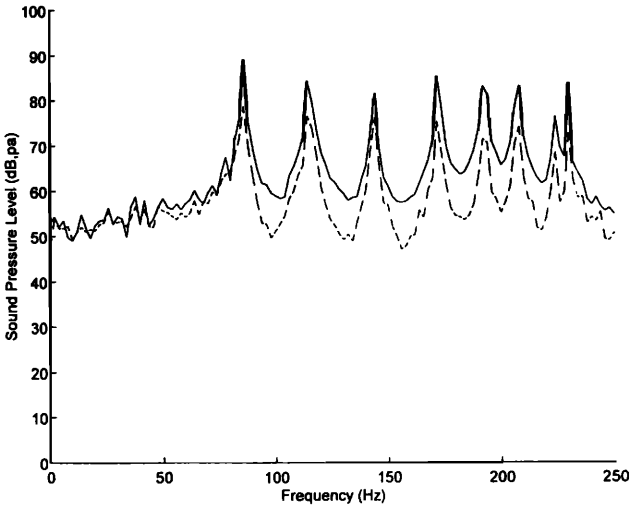

FIG. 14. Response spectrum of case 3 for the rectangular room problem (——— uncontrolled field; --- controlled field). Two microphones and two loudspeakers are employed to control the first four modes. The microphones and loudspeakers are collocated at (0.1, 0.2, 0.3) and (0.2, 0.7, 1.3 m), respectively. The Q:R ratio is selected to be 100:1.

a function of actuator locations. In case 2, if the control is imposed on only the first two modes, the first two resonance peaks are significantly attenuated, as shown in Fig. 13. However, the noise level of the (1,0,1) mode is increased because of the spillover effect.

In case 3, only two loudspeakers and two microphones are employed to control the enclosed noise field. The simulation result is shown in Fig. 14. In comparison with the reference case 1, less noise attenuation is obtained by using the reduced number of transducers. This situation is basically the same as that of the duct case.

In case 4, the loudspeakers are placed on the nodal plane of the (0,1,1) mode. The result in Fig. 15 shows that noise

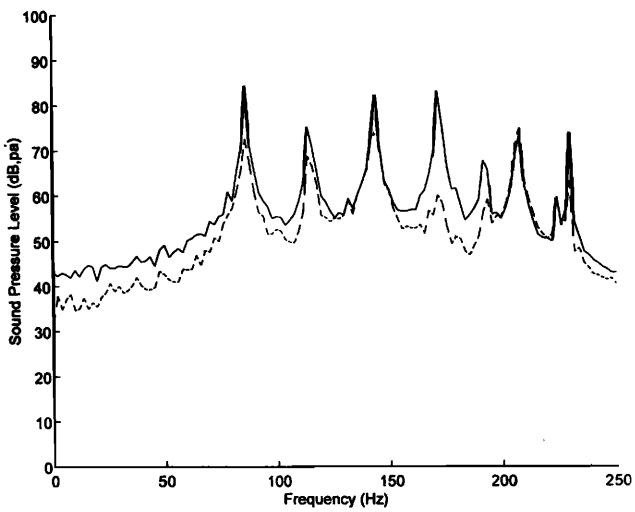

FIG. 15. Response spectrum of case 4 for the rectangular room problem (——— uncontrolled field; --- controlled field). Four microphones and four loudspeakers are employed to control the first four modes. The microphones are located at (0.1, 0.2, 0.3), (0.2, 0.7, 1.3), (0.15, 1.3, 1.6), and (0.9, 1.4, 1.9 m), respectively. The actuators are located at (0.1, 0.75, 0.8), (0.2, 0.7, 1), (0.5, 0.75, 1), and (0.9, 1.4, 1 m), respectively, which are on the nodal plane of mode (0,1,1). The Q:R ratio is selected to be 100:1.

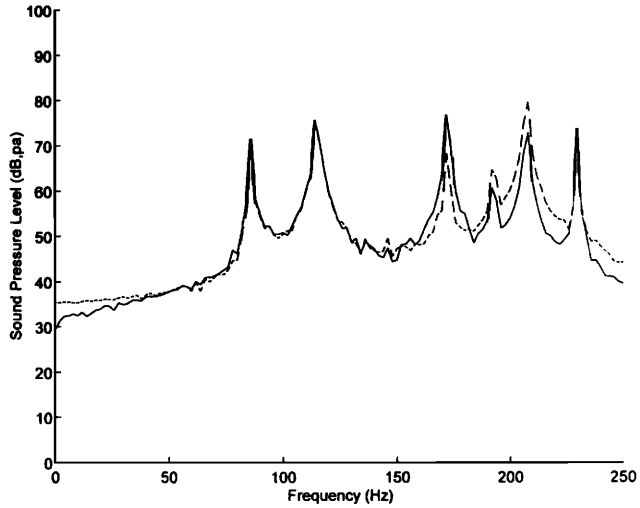

FIG. 16. Response spectrum of case 5 for the rectangular room problem (——— uncontrolled field; --- controlled field). Four microphones and four loudspeakers are employed to control the first four modes. The microphones are located at (0.1, 0.75, 0.8), (0.2, 0.7, 1), (0.5, 0.75, 1), and (0.9, 1.4, 1 m), respectively, which are on the nodal plane of mode (0,1,1). The loudspeakers are located at (0.1, 0.2, 0.3), (0.2, 0.7, 1.3), (0.15, 1.3, 1.6), and (0.9, 1.4, 1.9 m), respectively. The Q:R ratio is selected to be 100:1.

level of the (0,1,1) mode cannot be reduced because this mode appears uncontrollable to the controller for this particular loudspeaker arrangement. In case 5, the microphones are placed at the nodal plane of the (0,1,1) mode. Figure 16 shows a poor control performance and serious spillover because of the incomplete microphone measurement. Similar to the duct case, if the loudspeakers and the microphones are collocated, the control performance can be improved, as shown in Fig. 17. It can be concluded from these results of the rectangular room that similar behavior of the LQG-IMSC technique has occurred as that of the duct case. As a consequence, an increase of the dimensionality of the problem does not necessarily lead to an increase of the complexity of

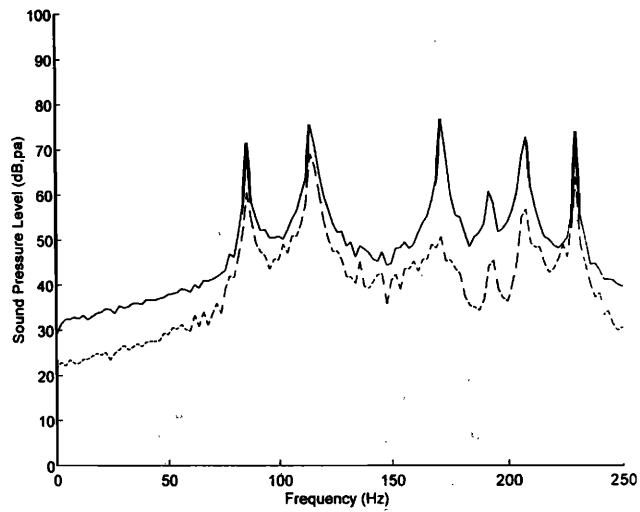

FIG. 17. Response spectrum of case 6 for the rectangular room problem (——— uncontrolled field; --- controlled field). Four microphones and four loudspeakers are employed to control the first four modes. The microphones and loudspeakers are collocated (0.1, 0.75, 0.8), (0.2, 0.7, 1), (0.5, 0.75, 1), and (0.9, 1.4, 1 m), respectively, which are on the nodal plane of mode (0,1,1). The Q:R ratio is selected to be 100:1.

Redistribution subject to ASA license or copyright; see http://acousticalsociety.org/content/terms. Download to IP: 140.113.38.11 On: Wed, 30 Apr 2014 06:45:39

the controller formulation. Of course, this statement is true only when the increase of the number of I/O channels in a hardware configuration required by a three-dimensional problem is not considered.

III. CONCLUSION

In this study, the LQG-IMSC algorithm is employed to control enclosed Gaussian noise fields. In IMSC, state feedback and estimation is carried out for each individual mode, which results in a simple formulation of controller design. Control gains are determined by the LQG algorithm that provides a proper weight (depending on the power rating of the loudspeaker) between the state of disturbance and expenditure of control energy. The simulation results of a duct and a rectangular room exhibit the effectiveness of the developed active noise canceler that provides global reduction of noise level in the enclosed fields.

Although an ideal IMSC algorithm requires distributed sensors and actuators, only discrete microphones and loudspeakers can be used in the ANC application. However, the simulation results indicate that good performance can possibly be achieved by using a moderate number of microphones and loudspeakers. When the number of microphones and the number of loudspeakers are both selected to be identical to the number of controlled modes, i.e., the transformation matrices in Eqs. (46) and (50) are both square, satisfactory control performance could be obtained. Naturally, this might limit the use of IMSC when one wishes to control many modes and an exceedingly large number of transducers might cause a potential problem in practical implementation. In addition, great care has to be taken not to place the microphones and loudspeakers right at or near the nodal points. Another problem that may arise in using discrete types of sensors and actuators is the spillover effect. This undesirable phenomenon may be alleviated by collocating the microphones and loudspeakers. Hardware implementation based on digital signal processors to verify the observation obtained from this simulation is currently under way.

ACKNOWLEDGMENT

The work was supported by the National Science Council in Taiwan, Republic of China, under Project No. NSC 83-0401-E-009-024.

[1] M. L. Munjal, *Acoustics of Ducts and Mufflers* (Wiley, New York, 1977).
[2] P. A. Nelson and S. J. Elliott, *Active Control of Sound* (Academic, London, 1992).
[3] H. Kwakernaak and R. Sivan, *Linear Optimal Control Systems* (Wiley–Interscience, New York, 1972).
[4] H. Öz and L. Meirovitch, "Stochastic independent modal space control of distributed-parameter systems," J. Optimization Theory Appl. **40**, 121–154 (1983).
[5] L. Meirovitch, *Dynamics and Control of Structures* (Wiley–Interscience, New York, 1990).
[6] M. J. Balas, "Trends in large space structure control theory: Fondest hope, widest dreams," IEEE Trans. Autom. Control **Ac-27**, 522–535 (1982).
[7] G. S. Nurre, R. S. Ryan, H. N. Scofield, and J. L. Sims, "Dynamics and control of large space structures," J. Guidance Control Dyn. **7**, 514–526 (1984).
[8] L. Meirovitch and H. Baruh, "Control of self-adjoint distributed parameter systems," J. Guidance Control Dyn. **15**, 60–66 (1982).
[9] L. Meirovitch and H. Öz, "Control of distributed gyroscopic systems," AIAA Pap. **78**, 330–340 (1978).
[10] M. J. Balas, "Active control of flexible systems," J. Optimization Theory Appl. **25**, 415–436 (1978).
[11] L. Meirovitch and L. M. Silverberg, "Globally optimal control of self-adjoint distributed systems," Optimal Control Appl. Methods **4**, 365–386 (1983).
[12] M. J. Grimble and M. A. Johnson, *Optimal Control and Stochastic Estimation, Theory and Applications* (Wiley, New York, 1988).
[13] A. E. Byson, Jr. and Y. C. Ho, *Applied Optimal Control* (Hemisphere, New York, 1981).
[14] B. D. O. Anderson and J. B. Moore, *Optimal Control, Linear Quadratic Methods* (Prentice-Hall, Englewood Cliffs, NJ, 1990).
[15] A. D. Pierce, *Acoustics: An Introduction to its Physical Principles and Applications* (Acoustic Society of America, Woodbury, NY, 1989).
[16] R. Haberman, *Elementary Applied Partial Differential Equations, with Fourier Series and Boundary Value Problems* (Prentice-Hall, Englewood Cliffs, NJ, 1987).
[17] L. Meirovitch and H. Baruh, "The implementation of modal filters for control of structures," J. Guidance Control Dyn. **8**, 707–716 (1985).
[18] K. K. Chew and M. Tomizuka, "Steady-state and stochastic performance of a modified discrete-time prototype repetitive controller," Trans. ASME J. Dyn. Syst. Meas. Control **112**, 35–41 (1990).

Redistribution subject to ASA license or copyright; see http://acousticalsociety.org/content/terms. Download to IP: 140.113.38.11 On: Wed, 30 Apr 2014 06:45:39